

Triplet superfluidity on a triangular ladder with dipolar fermions

Bradraj Pandey and Swapan K. Pati

Jawaharlal Nehru Centre for Advanced Scientific Research, Jakkur, Bangalore-560064, India

(Received 5 April 2016; revised manuscript received 16 November 2016; published 3 February 2017)

Motivated by recent experimental progress in the field of dipolar-Fermi gases, we investigate the quantum phases of dipolar fermions on a triangular ladder at half filling. Using density matrix renormalization group method, in the presence of onsite repulsion and intersite attractive interaction, we find an exotic spin-triplet superfluid phase in addition to the usual spin-density and charge-density waves. We examine the stability of the spin-triplet superfluid phase by varying hopping along the rungs of the triangle. The possibility of fermionic supersolidity has also been discussed, by considering three-body interaction in the Hamiltonian. We also study the effect of spin-dependent hopping on the stability of the spin-triplet superfluid phase.

DOI: [10.1103/PhysRevB.95.085105](https://doi.org/10.1103/PhysRevB.95.085105)

I. INTRODUCTION

Recent experimental advancements in the field of dipolar Fermi gases have given opportunity to explore the quantum phases of strongly correlated fermionic systems with long-range interactions [1,2]. The dipolar Fermi gas of ^{161}Dy [3] and fermionic polar molecules, $^{40}\text{K}^{87}\text{Rb}$ [4], $^{23}\text{Na}^{40}\text{K}$ [5], with large dipole moments have experimentally been realized in optical lattices. It has been found that the external electric and microwave fields on optical lattices can control quantum many-body interactions parameters of dipolar systems and polar molecules [6–9]. It has been argued that the long range and anisotropic characters of the dipolar interactions, in fact, can provide various types of exotic phases like charge-density wave (CDW); even though the density modulation is produced by charge neutral atoms or molecules, it is called CDW in the literature) [10–12], spin density wave [SDW; spin order for pseudo-spin-1/2 of dipolar fermions, shown in the schematic of Fig. 2(a)] [13,14], liquid-crystal [15,16], and conventional and unconventional fermionic superfluids [17–22], to name a few.

Finding phases like triplet superfluidity and triplet superconductivity is always very challenging and interesting too as these exotic phases have a connection to a number of topological phases and quantum computation. Interestingly, at low temperature, liquid ^3He forms fermionic superfluids, where ^3He atoms (or quasiparticles) form pairs with p -wave symmetry in the spin triplet state [23,24]. Chromium based quasi-one-dimensional superconductors [25,26] and strontium based oxide, Sr_2RuO_4 , are considered to be good candidates for triplet pairing [27,28].

Interestingly, ultra cold dipolar systems offer intriguing possibilities to explore unconventional pairing mechanisms of the condensed-matter system. For single component fermions, a dominant p_z -wave superfluidity has been proposed [17,18]. For two components fermions, it has been shown that there is a possibility of formation of both singlet and triplet superfluidity [29–31], as both singlet and triplet pairing are allowed in such systems. In a two-dimensional dipolar fermionic system, where dipoles are aligned with external electric field, it has been shown that p -wave superfluidity can be realized by varying anisotropy and geometry of the system [20]. Unconventional spin-density waves [14] and bond-order solids [32] have also been shown for the two-dimensional dipolar systems.

On the other hand, more exotic phases, like the supersolid phase, have been proposed for dipolar Fermi gas in a cubic optical lattice system [33]. Interestingly, in this, it has been shown that a p -wave superfluid is formed due to attractive interaction along the z direction and a charge-density wave in the XY plane due to electronic repulsions and together with the intermediate values of dipolar interactions. For a two-dimensional dipolar Fermi gas, coexistence of density-wave and p -wave superfluidity has been shown [34,35]. In a recent experimental study on ultra-cold three-dimensional optical lattice systems, the effect of multibody interaction has been demonstrated [36,37]. Furthermore, in a few numerical studies, it was shown that dominant three body Coulombic interactions can give rise to a host of interesting phases, like supersolid and bond-order phases [38–41]. Interestingly, for polar molecules in the optical lattice, the realization of three-body interactions using a microwave field has been proposed [42–44], and since then there have been various theoretical studies of microscopic models with three-body interactions [45–49]. These studies have shown that, with three body Coulombic interactions, the ground state can be quite exotic displaying quantum phases like topological phases, spin liquids, fractional quantum Hall states, etc.

Quasi-one-dimensional systems are quite unique. Due to strong quantum fluctuations, the true long range order is not possible for continuous symmetry breaking phases [50]. In a one-dimensional optical lattice, bosonization study has shown triplet superfluid (TSF) phase for dipolar fermions [51]. TSF phase is also found in two coupled one-dimensional systems for quadrupolar Fermi gas [13]. Interestingly, mixture of triplet and singlet superfluidity has also been shown in a quasi-one-dimensional system with two component fermions [52]. A recent DMRG study [53] has also found the TSF phase in a one-dimensional dipolar Fermi gas. In the presence of attractive head to tail arrangement of dipolar interactions, the one- and two-dimensional dipolar fermions become unstable and they undergo either collapse or phase separation. To overcome these difficulties, the bilayer system has been proposed, where dipoles are aligned perpendicular to the layers, giving more stable paired phases [54,55].

In this paper, we consider dipolar fermions in a triangular ladder system at half filling. We study the stability of various exotic phases, like, spin-density wave, charge density wave, and triplet-superfluid phases. In the ladder, the dipolar

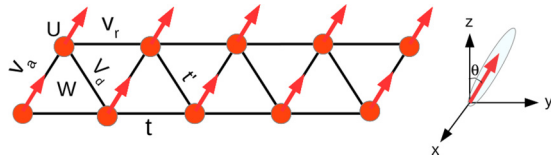


FIG. 1. Schematic of the triangular ladder with dipolar fermions (arrows indicate the directions of polarization of fermionic dipoles). There is onsite interaction U , attractive interaction V_a , repulsive interactions V_r , and V_d . The three-body interaction term is given as W and the hopping along the legs and rungs are represented as t and t' .

fermions are considered to be polarized along the rungs of the triangles (as shown in schematic of Fig. 1). The strength and direction of polarization can be controlled by external electric field or by varying distance between lattice sites. Due to alignment of dipolar fermions along the rungs, attractive interaction is generated on alternative rungs (odd rungs). It is also possible to generate repulsive interaction in each of the chains and diagonal rungs of the triangle, by alignment of dipoles. In the presence of attractive dipolar interaction and on-site Hubbard repulsion, a stable TSF phase gets generated. We have checked the stability of the TSF phase thoroughly, by tuning in the interchain hopping strength and the repulsive interaction parameters. Additionally, We have also examined the effect of spin-dependent interchain hopping on the stability of the TSF phase. Interestingly, due to triangular geometry, three-body interactions can also play an important role in identifying a new quantum phase like the fermionic super-solid phase of dipolar fermions [41].

The remaining part of the paper is organized as follows. In Sec. II we have discussed the model Hamiltonian and the method used to solve it. Subsequently, we have discussed the results obtained from DMRG calculations. This is divided into four subsections, where in each subsection the details of phase and phase transition are discussed. In the last section, we have summarized all our results.

II. THE MODEL

We consider two-component (pseudo-spin-1/2) dipolar fermions on a two-leg triangular ladder at half filling. The effective Hamiltonian of the system can be written as

$$H = - \sum_{\sigma,i} (t c_{\sigma,i}^\dagger c_{\sigma,i+2} + t' c_{\sigma,i}^\dagger c_{\sigma,i+1} + \text{H.c.}) + U \sum_i \hat{n}_{i,\uparrow} \hat{n}_{i,\downarrow} + \sum_{\langle i \neq j \rangle} V(i,j) \tilde{n}_i \tilde{n}_j - W \sum_i \tilde{n}_i \tilde{n}_{i+1} \tilde{n}_{i+2},$$

where $c_{\sigma,i}$ is the annihilation operator with spin $\sigma = \uparrow, \downarrow$ at site i . Here \uparrow and \downarrow states refer to two hyperfine states of dipolar atoms or molecules. $\tilde{n} = (n - \langle n \rangle)$, where n is the number operator and $\langle n \rangle = 1$. t and t' are the hopping terms and U is the onsite interaction term between the fermion with opposite spins; $V(i,j)$ is the two-body nearest-neighbor intersite interaction term. The last term in the Hamiltonian, W , represents attractive three-body interactions between the fermions, which act on the fermions belonging to the same triangle (as shown in the Fig. 1). The two-body interaction

term depends on direction and distance between the dipoles. When the two dipoles are parallel to each other, the interaction becomes repulsive, while when they align to each other along the rungs, interaction becomes attractive. The most dominating interactions arise from the nearest-neighbor terms [56,57], and also in optical lattice by adjusting the distance between sites, one can make other subdominating interactions quite smaller [57]. Thus, we restrict ourself to only nearest-neighbor terms of $V(i,j)$ in the Hamiltonian [41]. The two-body nearest-neighbor term, $V(i,j)$, can be described as

$$V(i,j) = \begin{cases} V_r & \text{Intersite repulsive term on each chain.} \\ V_d & \text{Intersite repulsive term for even rungs.} \\ -V_a & \text{Intersite attractive term for odd rungs.} \end{cases}$$

Since the dipolar interaction depends on angle and distance between the dipoles, it allows tuning of magnitude and sign of these interaction parameters to a wide range to explore rich quantum many-body phases. The dipolar interactions can be tuned by external electric field or changing the distance between sites. The above Hamiltonian preserves $U(1)$ and $SU(2)$ symmetry, which is related to conservation of total charge and spin degrees of freedom. Note that, for nonzero next nearest neighbor terms, t and W , the Hamiltonian does not have particle-hole symmetry.

To solve the above Hamiltonian and to find quantum phases in the parameter space, we have used the density-matrix renormalization group (DMRG) [58,59] method. We have used open boundary conditions and vary the DMRG cutoff (max = m) from 300 to 600, for consistency in results. Most of the results presented in the paper are obtained using max = 520, unless otherwise stated. To calculate the error, we have checked the truncation error, $e = 1 - \sum_i \rho_i$, where ρ_i is the eigenvalues corresponding to the reduced density matrix. We found that depending upon the interaction parameters and system size, truncation error e varies from 10^{-5} to 10^{-6} . We have verified energy and excitations for some parameters with those from exact diagonalization for smaller system sizes. To characterize different phases, namely SDW, TSF, and CDW phases, we have calculated corresponding correlation functions and also spin and charge density profiles. For showing plots of correlation functions, unless stated explicitly, we have considered system size $L = 128$. To determine phase boundary between different phases and to minimize the finite size effect, we have done finite-size scaling of order parameters, of the system with size (L) up to 160.

III. RESULTS

A. SDW to TSF to CDW transition

We first consider a simple case, where $t' = 0$, the intersite repulsive dipolar term, $V_r = 0$, $V_d = 0$, and the three-body term, $W = 0$. Due to the long range of dipolar interactions, two chains of triangular ladder can couple through attractive dipolar interaction V_a even though the tunneling between the chains remain zero [51]. For finding the TSF phase, we take onsite Hubbard interaction $U = 2$, and vary the attractive interaction V_a (0 to 4) along the rungs (odd rungs). For $U = 2$ and lower values of V_a , we find that to minimize repulsive onsite interaction, fermions stay put in each site and form spin density

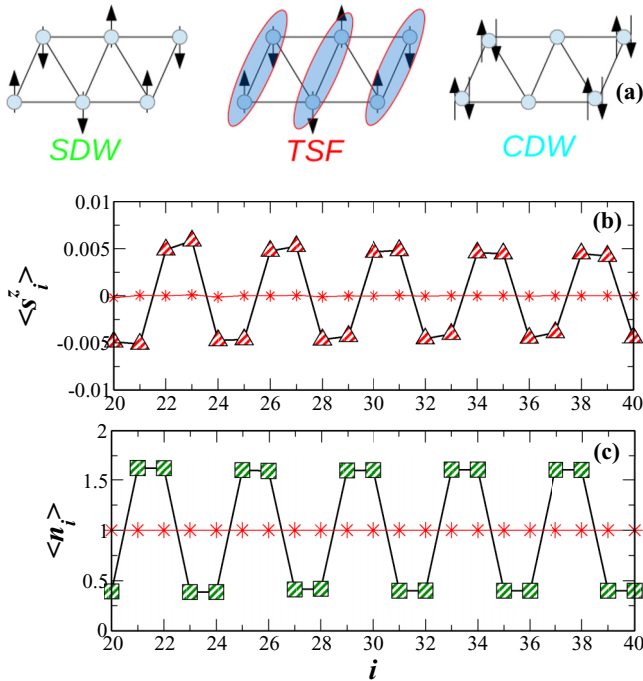


FIG. 2. (a) Schematic of the SDW, TSF, and CDW phases on a triangular lattice (here arrows indicate electronic spins of fermions). (b) Plot of spin-density ($\langle s_i^z \rangle$) with site index i , for $V_a = 1.6$ (triangle) and $V_a = 2.5$ (star). (c) Plot of charge density ($\langle n_i \rangle$) for $V_a = 2.4$ (star) and $V_a = 3.2$ (square).

wave, $|\uparrow, \uparrow, \downarrow, \downarrow, \uparrow, \uparrow, \downarrow, \downarrow, \uparrow, \uparrow, \dots\rangle$ [as shown in schematic of Fig. 2(a)]. In order to show the spin density profile of the system, in Fig. 2(b) we have plotted the spin-density ($\langle s_i^z \rangle$) of the system, with site index i . With an increase in attractive interaction, V_a , the fermions form intersite pairs along the rungs of the ladder, where the electronic spins form triplet symmetry ($|s^z = 0\rangle = |\uparrow\downarrow\rangle + |\downarrow\uparrow\rangle$) [60]. This phase remains so for moderate values of V_a . For a large value of attractive interaction, fermions with up and down spin prefer to sit together and form the CDW phase, where the state appears like, $|\uparrow\downarrow, \uparrow\downarrow, 0, 0, \uparrow\downarrow, \uparrow\downarrow, 0, 0, \dots\rangle$ [as shown in the schematic of Fig. 2(a)]. To show this, in Fig. 2(c), we have plotted charge density profile of fermions, $\langle n_i \rangle$, with site index i . Interestingly, this CDW phase appears even without any intersite-repulsive terms. This is precisely due to the triangular geometry and the attractive interaction along leg direction [61]. However, in the strictly one-dimensional case, for large values of attractive interaction, the system goes to either phase-separated phase or it collapses [53].

In order to characterize SDW, TSF, and CDW phases and their boundaries, we vary V_a with fixed value of $U = 2$, and we look into the behavior of corresponding correlation functions. For SDW phase, we have calculated correlation function, $S(r) = \langle s_i^z s_{i+r}^z \rangle$, where r (even distances) is the distance from the middle site of the ladder to the one end of the ladder. We found that with increase in r , fluctuations appears in the correlation function (Appendix Fig. 15). To reduce these fluctuations, we have calculated average correlation function, $S(r) = 1/N(r) \sum_r |\langle s_i^z s_{i+r}^z \rangle|$. Here, we have summed over all the correlations, which are separated by the same distance r

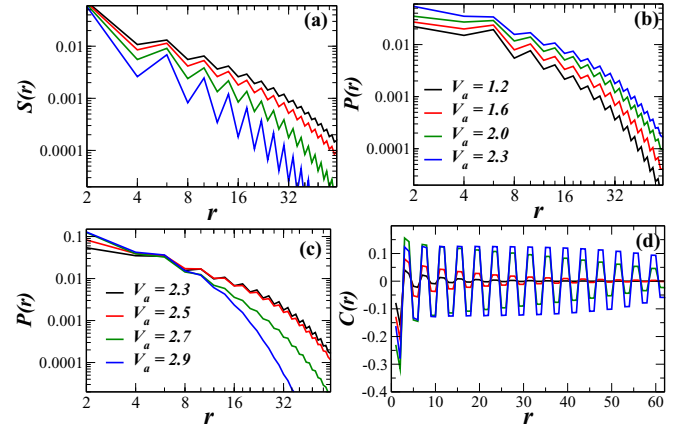


FIG. 3. (a) Plot of correlation function $S(r)$, (b) correlation function $P(r)$, for $U = 2$ and varying $V_a < 2.3$. (c) Plot of correlation function $P(r)$, (d) correlation function $C(r)$, for $U = 2$ and varying V_a (2.3 to 2.9).

from sites i and divided by the numbers $N(r)$ of such same distances correlations [62]. As shown in Fig. 3(a), for lower values of V_a , the correlation function $S(r)$ decays algebraically, while for larger values of $V_a \gtrsim 2.0$, it decays exponentially.

With an increase in attractive attraction along the rungs of the triangle, interchain fermions form bound pairs along the rung, giving rise to interchain spin-triplet superfluid phase, which is quite interesting. In general, the TSF phase can be characterized by pair correlation function [63–65] $P(r) = \langle \Delta_l^+ \Delta_{l+r} \rangle$, where $\Delta^\dagger(l) = (c_{i,\uparrow}^\dagger c_{i+1,\downarrow}^\dagger + c_{i,\downarrow}^\dagger c_{i+1,\uparrow}^\dagger)$ creates a fermionic pair in spin triplet state on a rung (labeled l) and r (even distance) is the distance from the rung l (near to the center of the triangular ladder). This correlation function $P(r)$, is also called p_z -wave-like superfluid correlation function, because of spin triplet pairing along the z direction. For $P(r)$ also, fluctuations appear with increase in r . To smooth out these fluctuations, we have calculated average correlation function, $P(r) = 1/N(r) \sum_r |\langle \Delta_l^+ \Delta_{l+r} \rangle|$, where we have summed over the correlations which are separated by the same distances r from rung l , divided by the numbers, $N(r)$, with such same distances correlations.

To characterize the phase boundary accurately between SDW and TSF phases, we have calculated the exponent of the correlation function, $S(r)$. The exponent K can be obtained by fitting the correlation function with algebraic decay function of the form, $S(r) \sim \cos(2k_F r)(1/r)^{1+K}$ [as shown in Fig. 4(c)] [66,67]. To get rid of short range correlation functions and the finite size effects, we have fitted the correlation function $S(r)$ from distance $r = 10$ to 70, for system size length $L = 160$. We find that the correlation function $S(r)$ fits very well in the SDW phase, however, near the phase boundary close to the TSF phases, the fitting error increases. From Luttinger liquid theory, for $K < 1$, the SDW phase dominates, while for $K > 1$, the TSF phase dominates [66–69]. The transition point for SDW to TSF phase is expected to be at $K = 1$. As shown in Fig. 4(b), at $V_a = 1.9 \pm 0.06$, the exponent K of the correlation function $S(r)$ takes the value $K \sim 1$, which signifies the transition from SDW phase to TSF phase.

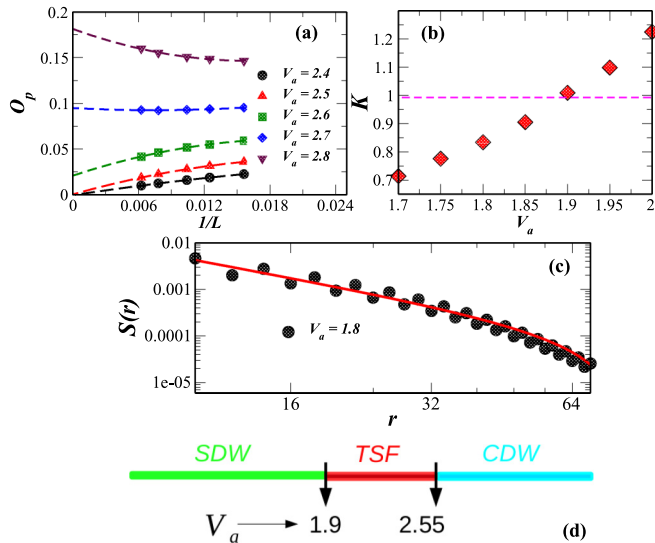


FIG. 4. Finite-size scaling of (a) order parameter O_p and (b) exponent K of the correlation function $S(r)$, at $U = 2$ and different values of V_a . (c) Power law fitting of $S(r)$ at $V_a = 1.6$, on a log-log scale for system size $L = 128$. (d) Phase diagram for fixed value of $U = 2$ with varying V_a .

To characterize the CDW phase, we have calculated the correlation function, $C(r) = \langle (n(i) - \bar{n})(n(j) - \bar{n}) \rangle$, where r is the distance from the middle site of the ladder to another on one side of the ladder. As shown in Fig. 3(d), the correlation function $C(r)$ for $V_a > 2.5$ has nearly long range order, while $P(r)$ decays exponentially [as shown in Fig. 3(c)]. Thus, for $V_a > 2.5$, the system is in the CDW phase. To calculate the phase boundary between *TSF* and *CDW* phase, we have done finite size scaling of the order parameter, $O_p = (1/L) \sum_{r=1}^L |C(r)|$. In the density wave phase order parameter O_p takes nonzero values in the thermodynamic limit [70]. To obtain the thermodynamic value of O_p , we have done finite-size scaling for systems with length L up to 160, by fitting the finite-size O_p values with a function, $O_p + O_1/L + O_2/L^2$. As shown in Fig. 4(a), *TSF* to *CDW* transition occurs at $V_a = 2.55 \pm 0.05$ as O_p takes finite nonzero values for $V_a = 2.55 \pm 0.05$. As shown in the schematic of Fig. 4(d), for fixed values of onsite interaction, $U = 2$ and by varying V_a , we found *SDW* phase for $V_a \lesssim 1.9$, *TSF* phase for $1.9 \lesssim V_a \lesssim 2.55$, and *CDW*-phase for $V_a \gtrsim 2.55$.

B. Effect of onsite repulsive interaction

To find the role of onsite interaction U in the triplet pairing and formation of other phases, we varied the U values from ($U = 0.0$ to 3.0), for fixed values of attractive interaction $V_a = 1.8$. As shown in Figs. 5(a) and 5(b), initially for lower values of U , the correlation function $C(r)$ shows nearly long range order, while $P(r)$ decays exponentially, indicating *CDW* phase in the system. On the other hand, for $U \gtrsim 1.1$, the correlation function $P(r)$ shows algebraic decay behavior, displaying *TSF* phase in the system. To find out the phase boundary between the *CDW* and *TSF* phase, we have done finite size scaling of order-parameter O_p . As shown in Fig. 6(a), O_p takes finite

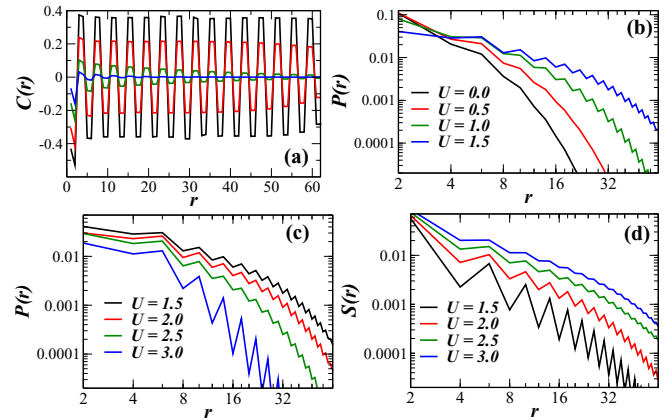


FIG. 5. (a) Plot of correlation function $C(r)$, (b) correlation function $P(r)$, for $V_a = 1.8$ and varying $U < 1.5$. (c) Plot of correlation function $P(r)$, (d) correlation function $C(r)$, for $V_a = 1.8$ and varying $U (1.5$ to $3.0)$.

nonzero values for $U = 1.1 \pm 0.05$, indicating the transition from *CDW* phase to *TSF* phase.

As shown in Figs. 5(c) and 5(d), with increase in U , initially $P(r)$ shows power law behavior, while $S(r)$ decays exponentially. On the other hand, for large values of U , $S(r)$ shows power law behavior, while $P(r)$ decays exponentially. For moderate values of U , *TSF* and *SDW* phases compete with each other. To find the phase boundary between *TSF* and *SDW* phase, we have done finite size scaling of exponent of correlation function $S(r)$, as discussed in the previous section. Figure 6(b) shows transition from *TSF* to *SDW* phase at $U = 1.9 \pm 0.06$, as the exponent of $S(r)$ takes the value $K = 1$. As shown in the schematic of Fig. 6(d), we find

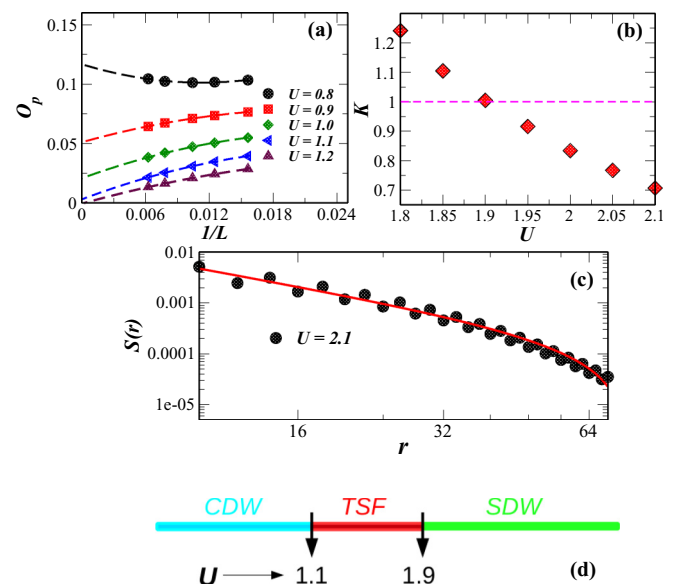


FIG. 6. Finite-size scaling of (a) order parameter O_p and (b) exponent K of the correlation function $S(r)$, at $V_a = 1.8$ and different values of U . (c) Power law fitting of $S(r)$ at $U = 2.2$, on a log-log scale, for $L = 128$. (d) Phase diagram for fixed value of $V_a = 1.8$ with varying U .

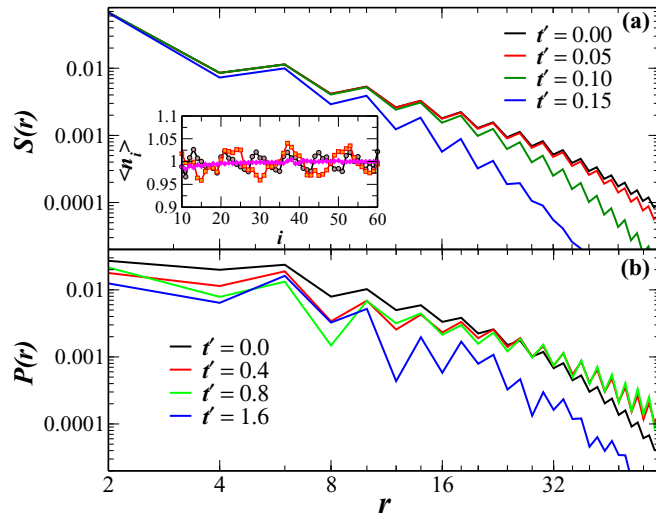


FIG. 7. (a) Plot of correlation function $S(r)$. (b) Plot of correlation function $P(r)$, as a function of r , at $U = 2$, $V_a = 1.6$, and varying t' (on a log-log scale). In the inset, charge density $\langle n_i \rangle$ is shown for $t' = 1.2$ (circle), 1.6 (square), and 2.4 (diamond).

the CDW phase for $U \lesssim 1.1$, TSF phase for $1.1 \lesssim U \lesssim 1.9$, and SDW phase for $U \gtrsim 1.9$, for a fixed value of attractive interaction, $V_a = 1.8$.

C. Effect of interchain hopping

Here, we study the effect of interchain hopping, t' on the triangular ladder. We find that, as the interchain hopping is turned on, the SDW phase becomes unstable and disappears quickly with increase in t' . On the other hand, TSF phase becomes prominent with nonzero t' values, however, as the t' becomes larger, the prominence decreases. The spin triplet pairs formed due to V_a term along the rung, get higher stability with the introduction of t' , as it promotes the antiferromagnetic exchange between the electrons on the rungs. This results in increase in pair correlation, $P(r)$. Interestingly, for large values of attractive interaction, V_a , when the system is in the CDW phase, it gets hardly affected by the interchain hopping term, as the charge ordered state arrests the effective hopping between the chains. However, close to the phase boundary between TSF and CDW phases, when the system is near the CDW phase boundary, for finite values of t' , the system can again make the transition to the TSF phase.

Now, using DMRG, we demonstrate the effect of t' by considering two values of V_a , 1.6 and 2.8, and for a fixed value of $U = 2$. These V_a values correspond to SDW and CDW phases, respectively, without any interchain hopping term t' . As we turn on t' , we look at the variation in SDW and CDW phases. As shown in Fig. 7(a), for $V_a = 1.6$, the spin-spin correlation function $S(r)$ starts decaying exponentially for $t' \gtrsim 0.1$ [Fig. 7(a)], whereas the pair correlation function $P(r)$ initially increases with t' , for even small values of it. It clearly shows that the system makes the transition from SDW phase to TSF phase in the presence of interchain hopping t' . On the other hand, as we increase the t' value, for larger values of t' ($t' \sim t$), the pair correlation function $P(r)$ starts decreasing [Fig. 7(b)]. Interestingly, there the system shows a density

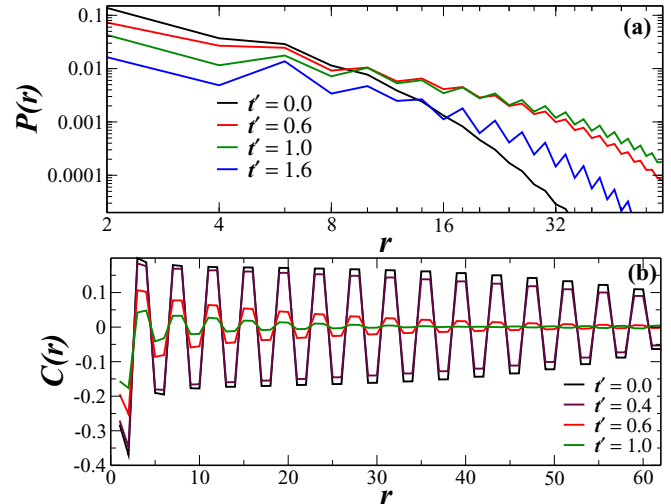


FIG. 8. (a) Plot of correlation function $P(r)$ as a function of r (on a log-log scale). (b) Plot of correlation function $C(r)$, as a function of r , at $U = 2.0$, $V_a = 2.8$ with different values of t' .

profile, $\langle n(i) \rangle$, which is oscillatory in nature [as shown in the inset of Fig. 7(a), for $t' = 1.2$ and 1.6]. In fact, at very large values of t' ($t' \gtrsim 2.0$), the system enters into a metallic phase, where the density becomes homogeneous and takes values around one [see inset of Fig. 7(a), for $t' = 2.4$].

We find that the CDW phase is quite robust against the interchain hopping term t' . As shown in Fig. 8(a), the charge-charge correlation function $C(r)$ shows nearly long range order for $t' \lesssim 0.5$. On the other hand, as shown in Fig. 8(b), the pair correlation function $P(r)$ decays exponentially for lower values of $t' \lesssim 0.5$, while it shows power law behavior for $t' > 0.5$. Such behavior of the correlation functions indicate a phase transition from CDW phase to TSF phase for $t' \simeq 0.55 \pm 0.05$. For moderate values of t' , the $P(r)$ shows power law behavior, while for larger values of $t' \gtrsim 1.2$, it starts decaying exponentially and the system again enters into a density wave phase. For large values of t' ($t' \sim 2.0$), the density wave phase enters into a metallic phase. For $V_a \gtrsim 3$, the CDW phase is quite stable and it requires a really large value of t' to destroy the CDW phase.

D. Effect of intersite repulsive interactions

When the dipolar fermions are aligned along the rungs of the triangle, repulsive interactions can be generated along each chain direction (V_r) as well as along the diagonal (V_d) of the triangular ladder (as shown in schematic Fig. 1). For demonstrating the effect of repulsive interactions, V_r and V_d , we chose interaction parameters $U = 2$, $t' = 0.4$, $V_a = 1.8$ and vary the intersite repulsive parameters V_r and V_d . As discussed in the previous section, in the absence of repulsive intersite interactions, for these parameter values, the system remains in the TSF phase. On the other hand, with an increase of intersite repulsive interactions, the fermions try to avoid each other and form a CDW state with structure, like $|2, 0, 0, 2, \dots\rangle$.

In Fig. 9, we have shown the effect of intersite repulsive interaction V_d , on the TSF phase keeping $V_r = 0$. As shown

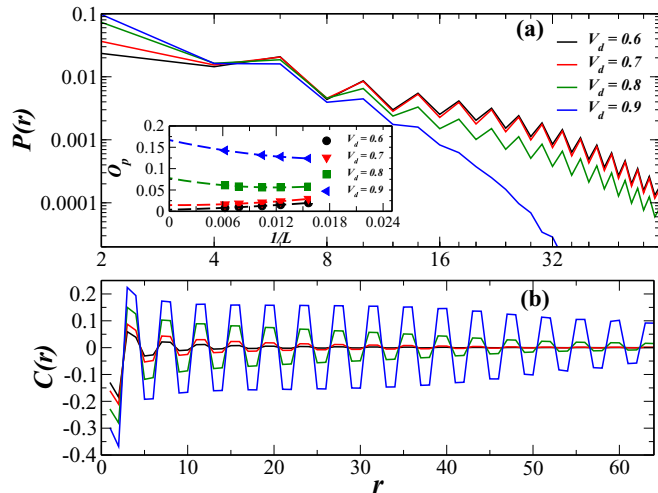


FIG. 9. (a) Plot of correlation function $P(r)$, as a function of r , at $U = 2.0$, $t' = 0.4$, $V_a = 1.8$, and different values of V_d . Inset shows finite size scaling of O_p with $1/L$. (b) Plot of correlation function $C(r)$, with distance r at $U = 2.0$, $t' = 0.4$, $V_a = 1.8$, and different values of V_d .

in Fig. 9(a), for lower values of $V_d < 0.8$, correlation function $P(r)$ shows power law behavior. For larger values of V_d , correlation function $C(r)$ shows nearly long range behavior [Fig. 9(b)]. To find the phase boundary between TSF and CDW, we have done finite size scaling of O_p . As shown in the inset of Fig. 9(a), O_p takes a small finite value for $V_d \sim 0.7$. In some cases, due to slow nature of transition and finite size effect, O_p can take very small nonzero values. So from the plot of the correlation function $C(r)$ [Fig. 9(b)] and finite size scaling of O_p , we have estimated the transition from TSF to CDW phase at $V_d = 0.75 \pm 0.06$.

In the presence of attractive interaction V_a , along the rungs of the triangles, the fermions in each of the chains become correlated with each other. We also found that in the presence of V_d , small values of repulsive interaction V_r are enough to produce a CDW phase [71]. As shown in Fig. 10(a), the pair correlation function $P(r)$ shows power law behavior up to $V_r \sim 0.24$, while for larger values of V_r , it decays exponentially. On the other hand, the charge charge correlation function $C(r)$ shows nearly long range behavior for $V_r \gtrsim 0.24$ [Fig. 10(b)]. To find the phase boundary, we have done finite size scaling of order parameter O_p . As shown in the inset of Fig. 10(a), O_p takes a finite value for $V_r = 0.24 \pm 0.02$, which clearly shows the phase transition from the TSF phase to the CDW phase at $V_r = 0.24 \pm 0.02$.

E. Effect of three-body interaction

Due to triangular geometry and dipolar interactions, an additional three-body interaction term may appear in each of the triangular plaquettes, as suggested by others on similar grounds [39,44]. The three-body term can break the particle hole symmetry of the Hamiltonian. In optical lattices, the three-body and two-body interactions can be tuned independently [42,43]. Here, we demonstrate the consequences of attractive three-body interaction [37,72], W , along with two-body interactions and ask whether the three-body term

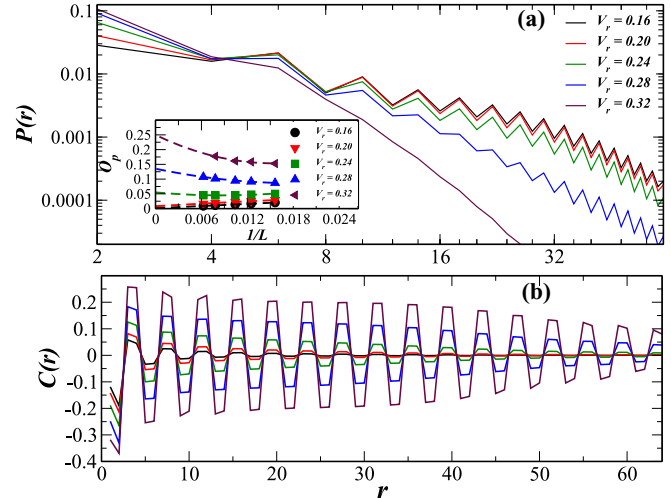


FIG. 10. Plot of correlation function (a) $P(r)$ as a function of r . (b) $C(r)$ as a function of r at $U = 2.0$, $t' = 0.4$, $V_a = 1.8$, $V_d = 0.3$, and different values of V_r . Inset shows finite size scaling of O_p with $1/L$.

can generate new phases or combine several phases. To show the effect of three-body interactions, we choose the system parameters, $U = 2$, $V_a = 1.8$, $V_d = 0.3$, $V_r = 0.1$, and $t' = 0.4$ and varied the W . Without the W term, the system exists in TSF phase for these parameters. As we turn on the attractive three-body interaction, W , both TSF and CDW phases coexist and the system remains so up to moderate values of W .

As shown in Fig. 11, the triplet pair correlation function $P(r)$, with an increase in W , shows power law behavior, with slight changes in exponent. Additionally, with an increase in W , a periodic modulation appeared in the charge correlation function $C(r)$. To see the appearance of CDW order in the thermodynamic limit, we have done finite size scaling of order parameter O_p . As shown in the inset of Fig. 12, O_p takes finite nonzero values for $W = 0.6 \pm 0.1$. Periodic modulation in density correlation $C(r)$ and algebraic decay of $P(r)$ gives a signature of fermionic supersolid phase in the system for

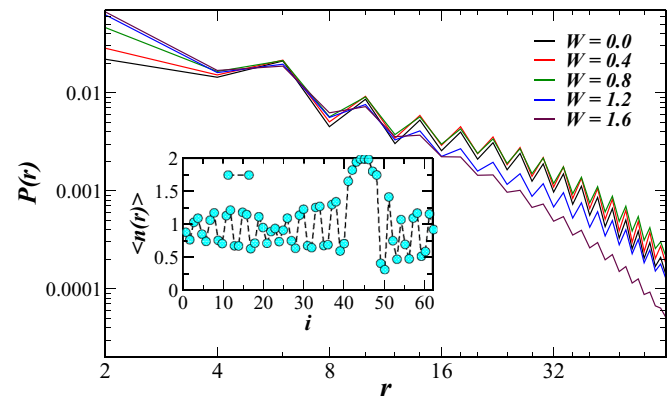


FIG. 11. Plot of correlation function $P(r)$ as a function of r , for interaction parameters $U = 2.0$, $V_a = 1.8$, $V_r = 0.1$, $V_d = 0.3$, $t' = 0.4$, and different values of W . Inset shows density profile of fermions $\langle n_i \rangle$, with site index i , for $W = 1.9$.

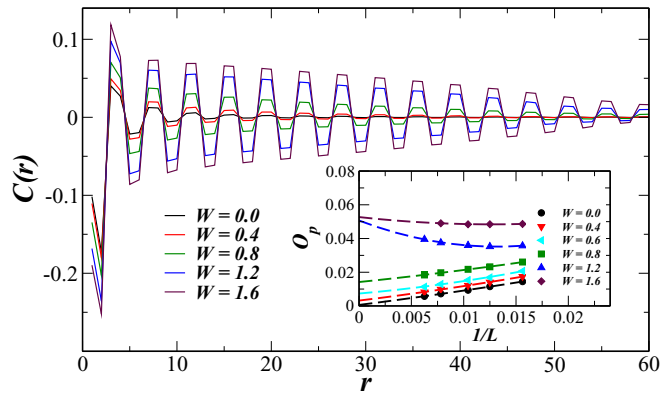


FIG. 12. Plot of correlation function $C(r)$ as a function of r , for interaction parameters, $U = 2.0$, $V_a = 1.8$, $V_r = 0.1$, $V_d = 0.3$, $t' = 0.4$, and different values of W . Inset shows finite size scaling of O_p with $1/L$.

$0.6 \lesssim W \lesssim 1.7$, where both CDW and TSF phases coexist. This supersolid phase is different from the supersolid phase formed due to coexistence of onsite pairing of fermions (s -wave superfluid) and a charge density wave of the system. Here, fermions form pairs in the spin-triplet state (p_x -wave superfluid), which coexist with the CDW phase of the system. For large values of $W \gtrsim 1.7$, the system becomes unstable and thereby become phase separated. In the phase separated state, density distribution is inhomogeneous, while correlation function $P(r)$ decay exponentially. Note that, in the phase separated state, there is generally a convergence problem, which we found for $W \gtrsim 2.0$. In the inset of Fig. 11, plot of charge density profile $\langle n_i \rangle$ has been shown for $W = 1.8$, with site index i (also see in Appendix Fig. 16, the plot of $\langle n_i \rangle$, for different values of W).

F. Effect of spin-dependent hopping

In this section, we analyze the effect of spin dependent hopping on the TSF phase. We apply spin dependent hopping along the rungs of the triangle. We considered the up-spin hopping term to be stronger than the down-spin hopping term [73]. The corresponding change in hopping term in the Hamiltonian can be written as

$$H_{t\sigma} = \sum_i (t'_\uparrow c_{i,\uparrow}^+ c_{i+1,\uparrow} + \text{H.c.}) + (\alpha t'_\downarrow c_{i,\downarrow}^+ c_{i+1,\downarrow} + \text{H.c.}),$$

where α is an anisotropic term [$\alpha = 1$ make the Hamiltonian the same as Eq. (1)]. The spin dependent hopping term breaks the spin rotational symmetry $SU(2)$ and also the time reversal symmetry of the Hamiltonian [50,74]. As the $SU(2)$ symmetry is broken, the ground state is no more in the $s_{tot}^z = 0$ sector, while the number sector is still fixed. In such a situation, we have checked our DMRG results with those from exact diagonalization results with the same setup for smaller system sizes. As the results compare fairly well, we have set up DMRG calculations with a fixed number of particles without considering the s_{tot}^z quantum number. Since the matrix dimension in each of the DMRG iterations increases quite considerably ($\sim 10^6$), we have carried out DMRG calculations with $\text{max} = 450$ and for system length $L = 96$. We have

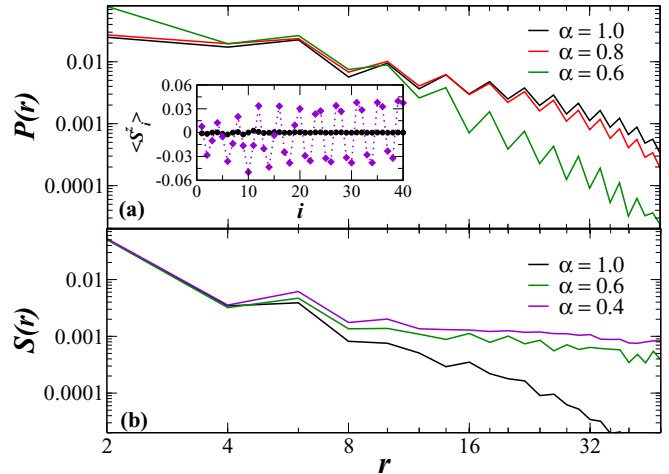


FIG. 13. (a) Plot of correlation function $P(r)$. (b) Correlation function $S(r)$, as a function of r , at $U = 2$, $V_a = 2.0$, $V_r = 0.1$, $V_d = 0.2$, and $t' = 0.4$, with varying α . Inset shows plot of spin density $\langle S_i^z \rangle$ with site index i , for $\alpha = 1$ (circle) and $\alpha = 0.4$ (diamond).

verified the results for $\alpha = 1$ by running DMRG calculations with $s_{tot}^z = 0$ and without considering s_{tot}^z quantum number up to $L = 96$ with $\text{max} = 450$ and found the results compare quite well. We thus have carried out DMRG calculations with the parameters, $U = 2$, $V_a = 2$, $V_r = 0.1$, $V_d = 0.2$, $t' = 0.4$ with varying α values. Note that for these parameter values with $\alpha = 1$, the system is known to be in TSF phase [see Fig. 13(a)].

With spin-dependent hopping, we find that the TSF phase is suppressed, while the SDW phase starts dominating. As shown in Fig. 13(a), the pair correlation function $P(r)$ decays algebraically for $\alpha \gtrsim 0.6 \pm 0.1$, showing clearly that the TSF phase is sustained by spin dependent hopping, while for $\alpha \lesssim 0.6 \pm 0.1$, the pair correlation decays exponentially. With lower values of α , spin-spin correlation function $S(r)$ has nearly quasi-long-range order for $\alpha \lesssim 0.6 \pm 0.1$ [Fig. 13(b)]. In the inset of Fig. 13(a), we show spin density profile, $\langle S_i^z \rangle$ with site index i . As can be seen, the $\langle S_i^z \rangle$ takes finite values for $\alpha = 0.4$, however, it vanishes for $\alpha = 1.0$. For lower values of α , the down spin becomes reluctant to hop between legs of the triangle, thus promoting SDW phase while suppressing TSF phase in the ladder system.

IV. CONCLUSION

In summary, we have investigated the SDW, TSF, and CDW phases of dipolar fermions, at half filling, on a triangular ladder. In the presence of moderate values of repulsive onsite interaction and attractive intersite interactions, the fermions form an exotic spin triplet superfluid phase. In the presence of intersite attractive interactions and onsite repulsive interaction, a charge density wave phase is found even without any intersite repulsive interactions. We have demonstrated the stability of the spin triplet phase, by introducing interleg hopping, which effectively enhances the spin triplet superfluid phase region by replacing the spin density wave phase. In the presence of

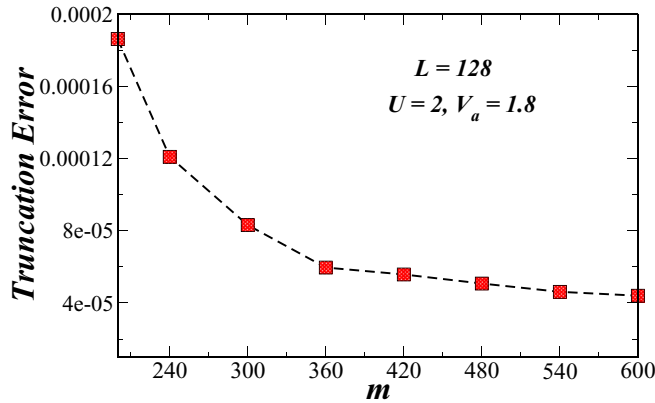


FIG. 14. Plot of truncation error with max values m , for interaction parameters $U = 2$, $V_a = 1.8$ (other parameters are kept zero).

repulsive interactions, we show the transition between TSF phase and a CDW phase. We also have looked at the effect of three-body interactions on the TSF and CDW phases. We find that the three-body term can introduce a fermionic supersolid phase, where both TSF and CDW coexist. We strongly believe that our study, which unravel the rich physics of exotic phases of dipolar-fermionic systems in ultra-cold systems would show inroads for further experiments.

ACKNOWLEDGMENTS

B.P. thanks the UGC, Govt. of India for support through a fellowship and S.K.P. acknowledges DST, Govt. of India for financial support.

APPENDIX

To check the accuracy of our DMRG calculations, we have calculated the truncation error of the system. In DMRG, the effective basis is truncated by keeping the m largest eigenvectors of the reduced density matrix corresponding to the m largest eigenvalues. The error caused by the truncation can be measured by calculating $e = 1 - \sum_i \rho_i$, where ρ_i is the eigenvalues corresponding to the reduced density matrix.

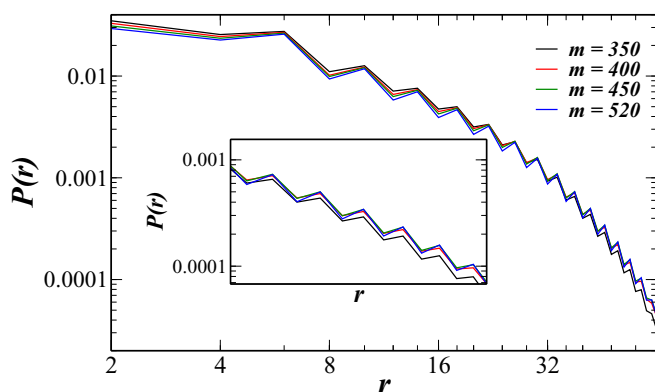


FIG. 15. Plot of correlation function $P(r)$ as a function of r , at $U = 2$, $V_a = 1.8$ (other parameters are kept zero), with different max values.

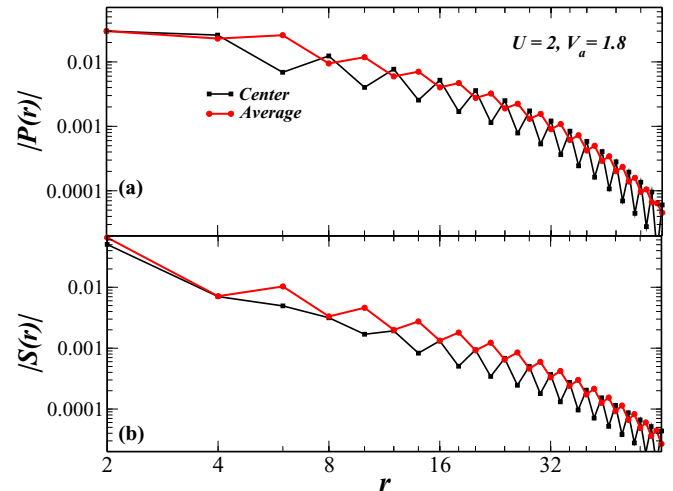


FIG. 16. Plot of correlation functions for interaction parameters $U = 2$, $V_a = 1.8$ (other parameters are kept zero). (a) $S(r)$ and (b) $P(r)$, in two different ways, one from the center of the lattice (square) and the second by taking an average (circle) for system size $L = 128$.

Figure 14 shows a plot of the truncation error with max values m , for system size $L = 128$ and for interaction parameters values $U = 2$, $V_a = 1.8$, keeping all the other parameters, t' , V_r , V_d , and W as zero. With increase in max value $m > 420$, the truncation error changes very slowly.

To check the behavior of correlation function $P(r)$ with max values, we have calculated the correlation function with different max values (Fig. 15). As shown in the inset of Fig. 15, $P(r)$ almost overlaps for $m = 450$ and $m = 520$. This proves that m value of 450 is large enough to obtain accurate correlation function $P(r)$.

We have used open boundary conditions for our calculations in DMRG. To remove the edge effects, we have computed correlation functions from a central site to one side of the triangular ladder. In case of correlation functions $S(r)$ and $P(r)$, we found that with an increase in distance r , rapid fluctuations appeared in correlation functions.

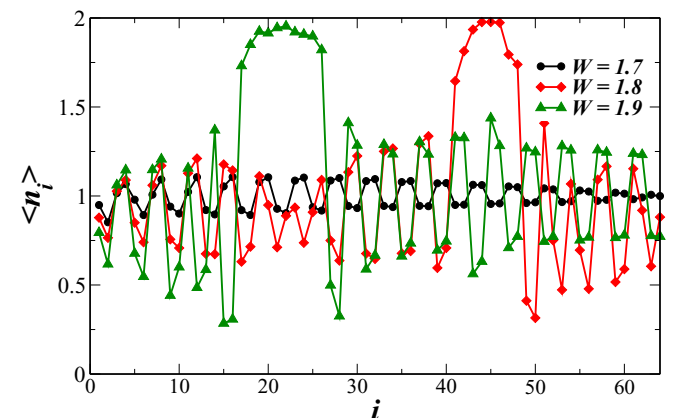


FIG. 17. Plot of charge density $\langle n_i \rangle$, for interaction parameters, $U = 2.0$, $V_a = 1.8$, $V_r = 0.1$, $V_d = 0.3$, $t' = 0.4$, and different values of W .

As shown in Fig. 16, to smoothen these fluctuations, we have calculated average correlation function, $S(r) = 1/N(r) \sum_r |(s_i^z s_{i+r}^z)|$, where we took the sum over the correlations, which are separated by the same distance r from the sites i from the other side of the ladder. This is then divided by the number, $N(r)$, of such same distance correlations. While averaging, we excluded lattice sites within a distance $L/4$ from both the ends of the ladder (of system size, L). We have calculated the average correlation function, $P(r) = 1/N(r) \sum_r |(\Delta_i^+ \Delta_{i+r})|$, by summing over the correlations, which are separated by the same distance r and dividing the sum by $N(r)$.

As discussed in Sec. III E, for large values of $W \gtrsim 1.7$, the system enters into a phase separated state. In Fig. 17, the plot of charge density profile $\langle n_i \rangle$ has been shown, for interaction parameters, $U = 2.0$, $V_a = 1.8$, $V_r = 0.1$, $V_d = 0.3$, $t' = 0.4$, and three different values of W . For $W = 1.7$, the system shows a periodic density modulation, while for $W = 1.8$, an inhomogeneous feature appears in the density profile. Interestingly, for $W = 1.8$, the $\langle n_i \rangle$ takes the maximum possible values (~ 2) near the center of the ladder, and for $W = 1.9$, it shifts to one side of the ladder. For $W \gtrsim 2.0$, we found a convergence problem.

-
- [1] A. Micheli, G. K. Brennen, and P. Zoller, *Nat. Phys.* **2**, 341 (2006).
- [2] T. Lahaye, C. Menotti, L. Santos, M. Lewenstein, and T. Pfau, *Rep. Prog. Phys.* **72**, 126401 (2009).
- [3] M. Lu, N. Q. Burdick, and B. L. Lev, *Phys. Rev. Lett.* **108**, 215301 (2012).
- [4] A. Chotia, B. Neyenhuis, S. A. Moses, B. Yan, J. P. Covey, M. Foss-Feig, A. M. Rey, D. S. Jin, and J. Ye, *Phys. Rev. Lett.* **108**, 080405 (2012); K. K. Ni, S. Ospelkaus, M. G. H. de Miranda, B. Pe'er, B. Neyenhuis, J. J. Zirbel, S. Kotochigova, P. S. Julienne, D. S. Jin, and J. Ye, *Science* **322**, 231 (2008).
- [5] C. H. Wu, J. W. Park, P. Ahmadi, S. Will, and M. W. Zwierlein, *Phys. Rev. Lett.* **109**, 085301 (2012).
- [6] M. Marinescu and L. You, *Phys. Rev. Lett.* **81**, 4596 (1998).
- [7] K.-K. Ni, S. Ospelkaus, D. Wang, G. Quémener, B. Neyenhuis, M. H. G. de Miranda, J. L. Bohn, J. Ye, and D. S. Jin, *Nature (London)* **464**, 1324 (2010).
- [8] L. Santos, G. V. Shlyapnikov, and M. Lewenstein, *Phys. Rev. Lett.* **90**, 250403 (2003).
- [9] I. Mourachko, W. Li, and T. F. Gallagher, *Phys. Rev. A* **70**, 031401(R) (2004).
- [10] M. M. Parish and F. M. Marchetti, *Phys. Rev. Lett.* **108**, 145304 (2012).
- [11] K. Mielsonson and J. K. Freericks, *Phys. Rev. A* **83**, 043609 (2011).
- [12] Y. Yamaguchi, T. Sogo, T. Ito, and T. Miyakawa, *Phys. Rev. A* **82**, 013643 (2010).
- [13] W.-M. Huang, M. Lahrz, and L. Mathey, *Phys. Rev. A* **89**, 013604 (2014).
- [14] S. G. Bhongale, L. Mathey, S.-W. Tsai, C. W. Clark, and E. Zhao, *Phys. Rev. A* **87**, 043604 (2013).
- [15] C. Lin, E. Zhao, and W. V. Liu, *Phys. Rev. B* **81**, 045115 (2010); **83**, 119901(E) (2011).
- [16] J. Quintanilla, S. T. Carr, and J. J. Betouras, *Phys. Rev. A* **79**, 031601(R) (2009).
- [17] L. You and M. Marinescu, *Phys. Rev. A* **60**, 2324 (1999).
- [18] M. A. Baranov, M. S. Mar'enko, V. S. Rychkov, and G. V. Shlyapnikov, *Phys. Rev. A* **66**, 013606 (2002).
- [19] T. Shi, J.-N. Zhang, C.-P. Sun, and S. Yi, *Phys. Rev. A* **82**, 033623 (2010).
- [20] G. M. Bruun and E. Taylor, *Phys. Rev. Lett.* **101**, 245301 (2008); **107**, 169901(E) (2011).
- [21] N. R. Cooper and G. V. Shlyapnikov, *Phys. Rev. Lett.* **103**, 155302 (2009).
- [22] B. Yan, S. A. Moses, B. Gadway, J. P. Covey, K. R. A. Hazzard, A. M. Rey, D. S. Jin, and J. Ye, *Nature (London)* **501**, 521 (2013).
- [23] D. Vollhardt and P. Woelfle, *Acta Phys. Polon. B* **31**, 2837 (2000).
- [24] A. J. Leggett, *Rev. Mod. Phys.* **47**, 331 (1975); **48**, 357(E) (1976).
- [25] J.-K. Bao, J.-Y. Liu, C.-W. Ma, Z.-H. Meng, Z.-T. Tang, Y.-L. Sun, H.-F. Zhai, H. Jiang, H. Bai, C.-M. Feng, Z.-A. Xu, and G.-H. Cao, *Phys. Rev. X* **5**, 011013 (2015).
- [26] X. Wu, F. Yang, C. Le, H. Fan, and J. Hu, *Phys. Rev. B* **92**, 104511 (2015).
- [27] A. P. Mackenzie and Y. Maeno, *Rev. Mod. Phys.* **75**, 657 (2003).
- [28] Y. Maeno, T. M. Rice, and M. Sigrist, *Phys. Today* **54**(1), 42 (2001).
- [29] C. Wu and J. E. Hirsch, *Phys. Rev. B* **81**, 020508(R) (2010).
- [30] R. Qi, Z.-Y. Shi, and H. Zhai, *Phys. Rev. Lett.* **110**, 045302 (2013).
- [31] K. Sun, C.-K. Chiu, H.-H. Hung, and J. Wu, *Phys. Rev. B* **89**, 104519 (2014).
- [32] S. G. Bhongale, L. Mathey, S.-W. Tsai, C. W. Clark, and E. Zhao, *Phys. Rev. Lett.* **108**, 145301 (2012).
- [33] T.-S. Zeng and L. Yin, *Phys. Rev. B* **89**, 174511 (2014).
- [34] Z. Wu, J. K. Block, and Georg M. Bruun, *Phys. Rev. B* **91**, 224504 (2015).
- [35] L. He and W. Hofstetter, *Phys. Rev. A* **83**, 053629 (2011).
- [36] M. Greiner, O. Mandel, T. Esslinger, T. W. Hänsch, and I. Bloch, *Nature (London)* **415**, 39 (2002).
- [37] S. Will, T. Best, U. Schneider, L. Hackermüller, D.-S. Lühmann, and I. Bloch, *Nature (London)* **465**, 197 (2010).
- [38] Z.-K. Lu, Y. Li, D. S. Petrov, and G. V. Shlyapnikov, *Phys. Rev. Lett.* **115**, 075303 (2015).
- [39] X.-F. Zhang, Y.-C. Wen, and Y. Yu, *Phys. Rev. B* **83**, 184513 (2011).
- [40] B. Capogrosso-Sansone, S. Wessel, H. P. Büchler, P. Zoller, and G. Pupillo, *Phys. Rev. B* **79**, 020503(R) (2009).
- [41] T. Mishra, S. Greschner, and L. Santos, *Phys. Rev. A* **91**, 043614 (2015).
- [42] H. P. Büchler, A. Micheli, and P. Zoller, *Nat. Phys.* **3**, 726 (2007).
- [43] K. P. Schmidt, J. Dorier, and A. M. Läuchli, *Phys. Rev. Lett.* **101**, 150405 (2008).
- [44] L. Bonnes and S. Wessel, *Phys. Rev. B* **83**, 134511 (2011).
- [45] R. D. Murphy and J. A. Barker, *Phys. Rev. A* **3**, 1037 (1971).
- [46] N. R. Cooper, *Phys. Rev. Lett.* **92**, 220405 (2004).

- [47] D. S. Petrov, *Phys. Rev. A* **67**, 010703(R) (2003).
- [48] A. Wójs, C. Töke, and J. K. Jain, *Phys. Rev. Lett.* **105**, 196801 (2010).
- [49] J. K. Pachos and M. B. Plenio, *Phys. Rev. Lett.* **93**, 056402 (2004).
- [50] M. A. Cazalilla, A. F. Ho, and T. Giamarchi, *Phys. Rev. Lett.* **95**, 226402 (2005).
- [51] T. N. De Silva, *Phys. Lett. A* **377**, 871 (2013).
- [52] S. Uchino, A. Tokuno, and T. Giamarchi, *Phys. Rev. A* **89**, 023623 (2014).
- [53] H. Mosadeq ans R. Asgari, *Phys. Rev. B* **91**, 085126 (2015).
- [54] A. C. Potter, E. Berg, Daw-Wei Wang, B. I. Halperin, and E. Demler, *Phys. Rev. Lett.* **105**, 220406 (2010).
- [55] D.-W. Wang, M. D. Lukin, and E. Demler, *Phys. Rev. Lett.* **97**, 180413 (2006).
- [56] C. Trefzger, C. Menotti, and M. Lewenstein, *Phys. Rev. Lett.* **103**, 035304 (2009).
- [57] X. Li and W. V. Liu, *Phys. Rev. A* **87**, 063605 (2013).
- [58] S. R. White, *Phys. Rev. Lett.* **69**, 2863 (1992); *Phys. Rev. B* **48**, 10345 (1993).
- [59] U. Schollwöck, *Rev. Mod. Phys.* **77**, 259 (2005).
- [60] A. Romano, P. Gentile, C. Noce, I. Vekhter, and M. Cuoco, *Phys. Rev. B* **93**, 014510 (2016).
- [61] F. M. Marchetti and M. M. Parish, *Phys. Rev. B* **87**, 045110 (2013).
- [62] M. Guerrero, G. Ortiz, and J. E. Gubernatis, *Phys. Rev. B* **62**, 600 (2000).
- [63] M. Tezuka, R. Arita, and H. Aoki, *Phys. Rev. B* **76**, 155114 (2007).
- [64] S. Uchino and T. Giamarchi, *Phys. Rev. A* **91**, 013604 (2015).
- [65] F. Iemini, T. O. Maciel, and R. O. Vianna, *Phys. Rev. B* **92**, 075423 (2015).
- [66] L. Arrachea, A. A. Aligia, E. Gagliano, K. Hallberg, and C. Balseiro, *Phys. Rev. B* **50**, 16044 (1994); **52**, 9793(E) (1995).
- [67] M. Troyer, H. Tsunetsugu, T. M. Rice, J. Riera, and E. Dagotto, *Phys. Rev. B* **48**, 4002 (1993).
- [68] K. Penc and F. Mila, *Phys. Rev. B* **49**, 9670 (1994).
- [69] R. T. Clay, A. W. Sandvik, and D. K. Campbell, *Phys. Rev. B* **59**, 4665 (1999).
- [70] Y. Z. Zhang, *Phys. Rev. Lett.* **92**, 246404 (2004).
- [71] B. Pandey, S. Sinha, and S. K. Pati, *Phys. Rev. B* **91**, 214432 (2015).
- [72] T. Sowiński, *Phys. Rev. A* **85**, 065601 (2012).
- [73] W. V. Liu, F. Wilczek, and P. Zoller, *Phys. Rev. A* **70**, 033603 (2004).
- [74] Y.-H. Liu and L. Wang, *Phys. Rev. B* **92**, 235129 (2015).